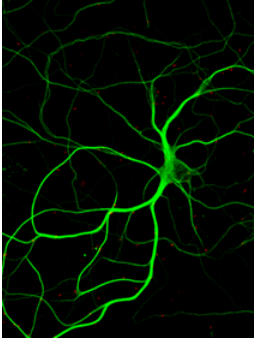


Neuroscience 2023 Scientific Imagery

Store Items

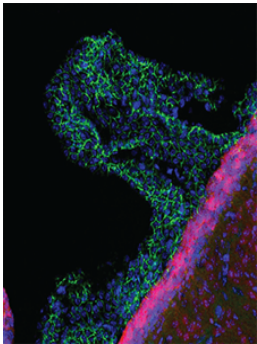
COASTERS



Description: This image shows interaction between the tau protein and protein phosphatase 1 (PP1) in a cultured rat hippocampal neuron. The neuron is stained for β -III tubulin (green) and the red puncta represent co-localization of individual tau and PP1 molecules as determined by proximity ligation assay. The functional interaction between these molecules has implications for axonal transport dysregulation in Alzheimer's disease and other tauopathies.

Credits: Benjamin Combs, Kyle R. Christensen, Collin Richards, Andrew Kneynsberg, Rebecca L. Mueller, Sarah L. Morris, Gerardo A. Morfini, Scott T. Brady and Nicholas M. Kanaan

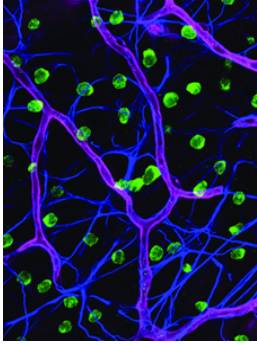
Journal of Neuroscience 10 November 2021, 41 (45) 9431-9451; DOI: <https://doi.org/10.1523/JNEUROSCI.1914-20.2021>



Description: This image shows GFAP-Cre activity (tdTomato/red) in a choroid plexus (marked by β -catenin/green) of a lateral ventricle of mouse brain at postnatal day 7.

Credits: Kong-yan Wu, Fu-lei Tang, Daehoon Lee, Yang Zhao, Hyunjin Song, Xiao-Juan Zhu, Lin Mei and Wen-Cheng Xiong

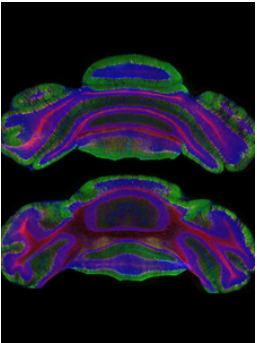
Journal of Neuroscience 6 May 2020, 40 (19) 3862-3879; DOI: <https://doi.org/10.1523/JNEUROSCI.1520-19.2020>



Description: This image shows the neurovascular unit of the retina, including capillaries (magenta), astroglia (blue), and cholinergic amacrine cells (green).

Credits: Elena Ivanova, Tamas Kovacs-Oller and Botir T. Sagdullaev

Journal of Neuroscience 9 August 2017, 37 (32) 7580-7594; DOI:
<https://doi.org/10.1523/JNEUROSCI.0187-17.2017>

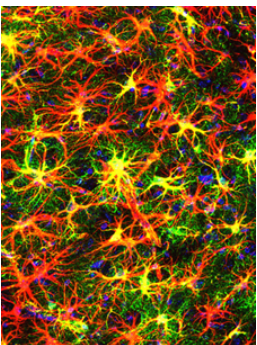


Description: This image shows the patterned degeneration seen in coronal cerebellums of 10-month-old mice that have lost Ankyrin-R in the CBS. Purkinje neurons are labeled for Calbindin (green) and Neurofilament-H (red), and nuclei are in blue (Hoechst).

Credits: Sharon R. Stevens, Meike E. van der Heijden, Yuki Ogawa, Tao Lin, Roy V. Sillitoe and Matthew N. Rasband

Journal of Neuroscience 5 January 2022, 42 (1) 2-15; DOI:
<https://doi.org/10.1523/JNEUROSCI.1132-21.2021>

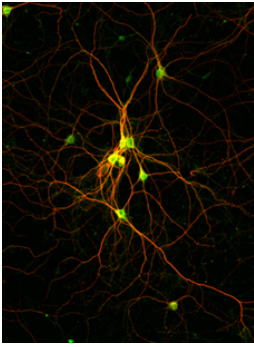
SOCKS



Description: Immunohistochemistry for astrocyte-specific GCaMP6f (green), glial fibrillary acidic protein (GFAP; red), and DAPI (blue). This technique was used to analyze the overlap (yellow) between the GCaMP6f and astrocytes in the basolateral amygdala (BLA) to ensure selective expression for fiber photometry recordings during fear learning.

Credits: Rebecca L. Suthard, Ryan A. Senne, Michelle D. Buzharsky, Angela Y. Pyo, Kaitlyn E. Dorst, Anh H. Diep, Rebecca H. Cole and Steve Ramirez

Journal of Neuroscience 5 July 2023, 43 (27) 4997-5013; DOI:
<https://doi.org/10.1523/JNEUROSCI.1775-22.2023>

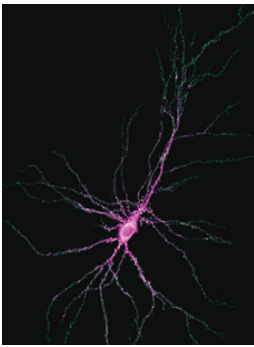


Description: The image shows cultured neurons from mouse cortex labeled with the dendritic marker protein MAP-2 (red) and the protein kinase SLK (green). In neuronal cells, SLK regulates the formation of the distal dendritic tree and the stabilization of inhibitory synapses.

Credits: Susanne Schoch, Anne Quatraccioni, Barbara K. Robens, Robert Maresch, Karen M.J. van Loo, Silvia Cases-Cunillera, Tony Kelly, Thoralf Opitz, Valeri Borger, Dirk Dietrich, Julika Pitsch, Heinz Beck and Albert J. Becker

Journal of Neuroscience 29 September 2021, 41 (39) 8111-8125; DOI:
<https://doi.org/10.1523/JNEUROSCI.0352-21.2021>

TUMBLER

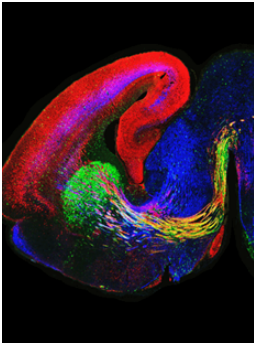


Description: This image shows the synaptic distribution of the synaptic Ras/Rap GAP SynGAP (green) in an mCherry-labeled hippocampal pyramidal cell (magenta) in culture.

Credits: Timothy R. Gamache, Yoichi Araki and Richard L. Huganir

Journal of Neuroscience 19 February 2020, 40 (8) 1596-1605; DOI:
<https://doi.org/10.1523/JNEUROSCI.0420-19.2020>

WATER BOTTLE

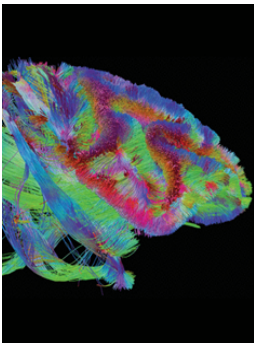


Description: This image of an embryonic day 18.5 mouse brain shows malformations in the striatal direct pathway (green), the corticofugal pathway (red), and the thalamocortical pathway (blue) that occur when the transcription factor *Isl1* is conditionally inactivated within the ventral forebrain.

Credits: Jacqueline M. Ehrman, Paloma Merchan-Sala, Lisa A. Ehrman, Bin Chen, Hee-Woong Lim, Ronald R. Waclaw and Kenneth Campbell

Journal of Neuroscience 20 April 2022, 42 (16) 3344-3364; DOI: <https://doi.org/10.1523/JNEUROSCI.2291-21.2022>

COLOR CHANGING MUG



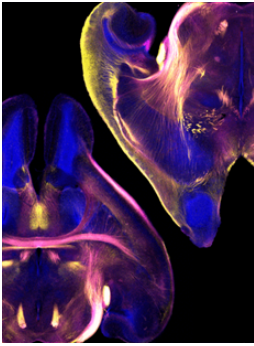
Description: This image shows tractography reconstructions of frontal white matter pathways in the macaque brain. Tractography enables us to compare human and non-human primate frontal white matter networks, showing disproportionate volume increases in humans for certain tracts associated with language and higher cognitive functions.

Credits: Rachel L. C. Barrett, Matthew Dawson, Tim B. Dyrby, Kristine Krug, Maurice Ptito, Helen D'Arceuil, Paula L. Croxson, Philippa J. Johnson, Henrietta Howells, Stephanie J. Forkel, Flavio Dell'Acqua and Marco Catani

Journal of Neuroscience 4 March 2020, 40 (10) 2094-2107; DOI: <https://doi.org/10.1523/JNEUROSCI.1650-18.2019>

Swag

STICKY NOTES

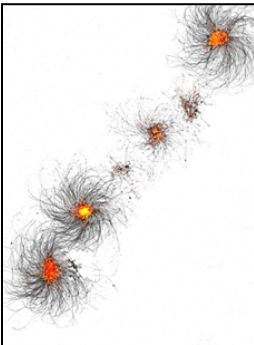


Description: This image shows horizontal brain sections from a neonatal wild-type mouse (bottom left) and a Tbr1 knockout mouse (top right), immunostained for the axon markers L1 (magenta) and neurofilament medium chain (yellow) with a nuclear counterstain (blue). Homozygous Tbr1 mutation causes severe axon tract defects and upregulation of neurofilament.

Credits: Marissa Co, Rebecca A. Barnard, Jennifer N. Jahncke, Sally Grindstaff, Lev M. Fedorov, Andrew C. Adey, Kevin M. Wright and Brian J. O'Roak

Journal of Neuroscience 14 September 2022, 42 (37) 7166-7181; DOI:

<https://doi.org/10.1523/JNEUROSCI.0409-22.2022>



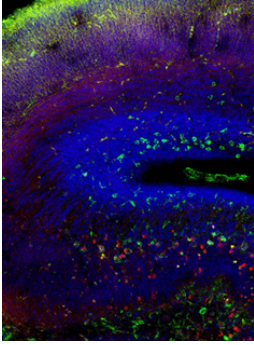
Description: This image shows several cerebellar migratory neuron aggregates 24 hours after plating. The neurons are depleted of mitotic motor, KIFC1 and stained with β -III tubulin (black) and DAPI (yellow-orange). Concentrated presence of neurons in the aggregate forms an intense yellow-orange signal and as neurons migrate out of the aggregate, the intensity of this signal subsidizes. But even after 24 hours, far fewer cells migrated out from the aggregate due to the inability of the neuron to directionally migrate out from the aggregates in the absence of KIFC1.

Credits: Hemalatha Muralidharan, Shrobona Guha, Kiran Madugula, Ankita Patil, Sarah A. Bennison, Xiaohuan Sun, Kazuhito Toyo-oka and Peter W. Baas

Journal of Neuroscience 16 March 2022, 42 (11) 2149-2165; DOI:

<https://doi.org/10.1523/JNEUROSCI.1708-21.2022>

LIP BALM

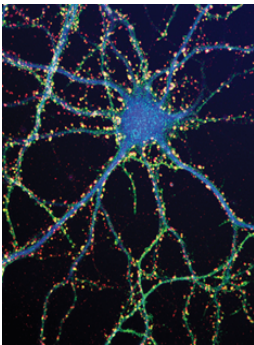


Description: Munc 18-1 knock-out mouse brain (E18) showing cellular stress response in hippocampus and cortex by phosphorylated p53 staining (green) and cell death in the hippocampus marked by fragmented cleaved caspase 3 (red) positive nuclei (DAPI in blue).

Credits: Femke M. Feringa, Annemiek A. van Berkel, Anushka Nair and Matthijs Verhage

Journal of Neuroscience 18 January 2023, 43 (3) 347-358; DOI:
<https://doi.org/10.1523/JNEUROSCI.0611-22.2022>

MAGNET

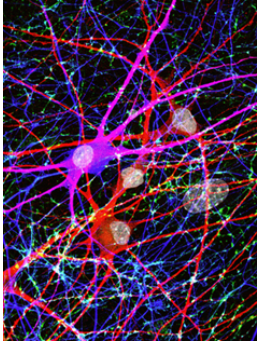


Description: This hippocampal neuron, 14 d *in vitro*, lacks NMDA receptor subunit GluN2B. It was immunostained for the AMPA receptor subunit GluA1 (green), the vesicular glutamate transporter VGLUT1 (red), and the microtubule-associated protein MAP2 (blue). An edge-detect filter was used to enhance color and cluster contour. In the absence of the GluN2B subunit, synaptic clustering of AMPA receptors is increased as a result of impaired anchoring of the synaptic proteasome.

Credits: Joana S. Ferreira, Jeannette Schmidt, Pedro Rio, Rodolfo Águas, Amanda Rooyackers, Ka Wan Li, August B. Smit, Ann Marie Craig and Ana Luisa Carvalho

Journal of Neuroscience 3 June 2015, 35 (22) 8462-8479; DOI:
<https://doi.org/10.1523/JNEUROSCI.3567-14.2015>

JOURNAL

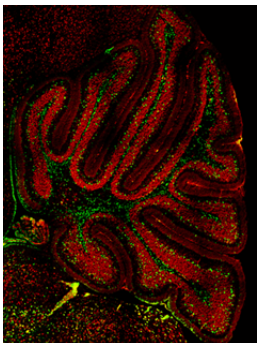


Description: This confocal image depicts neurons that were derived from human stem cells and sparsely infected with lentivirus expressing EGFP (blue). Nuclei were labeled with DAPI (white), dendrites labeled with antibodies against MAP2 (red), and synapses labeled with antibodies against synapsin (green). These neurons were used to assess phenotypes resulting from a mutation in the synaptic organizing protein Neuroligin-4.

Credits: Thomas P. Cast, Daniel J. Boesch, Kim Smyth, Alisa E. Shaw, Michael Ghebrial and Soham Chanda

Journal of Neuroscience 20 January 2021, 41 (3) 392-407; DOI:
<https://doi.org/10.1523/JNEUROSCI.0404-20.2020>

LANYARDS

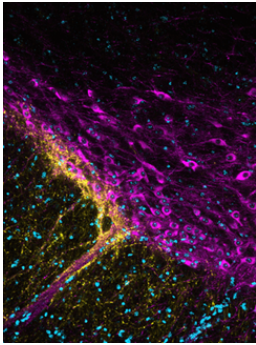


Description: The image shows a postnatal mouse cerebellum stained for Pax2 (green) and NeuN (red), highlighting immature inhibitory interneurons and excitatory granule cells, respectively. Shh signaling promotes the expansion of Pax2 progenitors that contribute selectively to the stellate cell pool, one of two molecular layer interneuron subtypes.

Credits: Wen Li, Lei Chen, Jonathan T. Fleming, Emily Brignola, Kirill Zavalin, Andre Lagrange, Tonia Rex, Shane A. Heiney, Gregory J. Wojaczynski, Javier F. Medina and Chin Chiang

Journal of Neuroscience 29 June 2022, 42 (26) 5130-5143; DOI:
<https://doi.org/10.1523/JNEUROSCI.2073-21.2022>

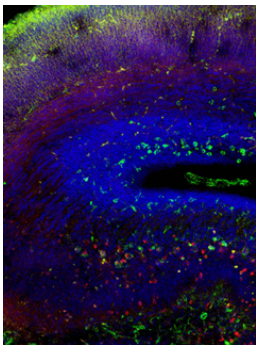
Digital Signage



Description: Channelrhodopsin-expressing fibers (yellow) from insular cortex dynorphin (DYN) neurons traverse striosome-dendron bouquets to contact dopamine neurons (magenta) in the substantia nigra pars compacta. DAPI is shown in cyan. In this issue, Pina et al show that insular cortex DYN neurons serve as a driving force in the escalated intake that occurs following prolonged alcohol drinking. As shown here, insula DYN neurons send long-range projections to the substantia nigra, suggesting a possible downstream mechanism underlying their role in escalated alcohol intake.

Credits: Melanie M. Pina, Dipanwita Pati, Sofia Neira, Lisa R. Taxier, Christina M. Stanhope, Alexandra A. Mahoney, Shannon D'Ambrosio, Thomas L. Kash and Montserrat Navarro

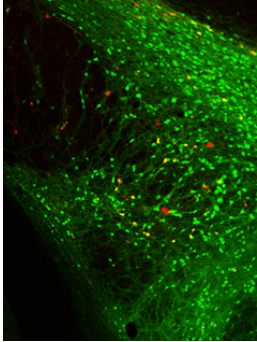
Journal of Neuroscience 12 July 2023, 43 (28) 5158-5171; DOI:
<https://doi.org/10.1523/JNEUROSCI.0406-22.2023>



Description: Munc 18-1 knock-out mouse brain (E18) showing cellular stress response in hippocampus and cortex by phosphorylated p53 staining (green) and cell death in the hippocampus marked by fragmented cleaved caspase 3 (red) positive nuclei (DAPI in blue).

Credits: Femke M. Feringa, Annemiek A. van Berkel, Anushka Nair and Matthijs Verhage

Journal of Neuroscience 18 January 2023, 43 (3) 347-358; DOI:
<https://doi.org/10.1523/JNEUROSCI.0611-22.2022>



Description: The presynaptic LH GABA-ergic neurons which dominate VTA GABA-ergic neurons were labeled by the EGFP and DsRed simultaneously. LH, lateral hypothalamus; VTA, ventral tegmental area.

Credits: Yu Ma, Weinan Zhao, Dandan Chen, Dongyu Zhou, Yihong Gao, Yixin Bian, Yuqing Xu, Sun-Hui Xia, Tantan Fang, Jun-Xia Yang, Lingzhen Song, He Liu, Hai-Lei Ding, Hongxing Zhang and Jun-Li Cao

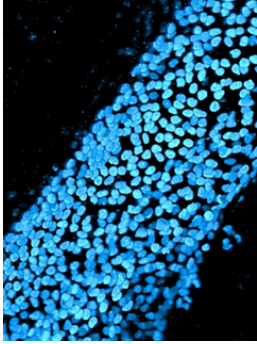
Journal of Neuroscience 14 June 2023, 43 (24) 4525-4540; DOI:
<https://doi.org/10.1523/JNEUROSCI.2298-22.2023>



Description: Surface view of a neonatal mouse cochlea, from tiled confocal projection images. Mechanosensory hair cells are labeled with Myosin VIIa, magenta, and a subset of supporting cells are labeled with Fatty acid binding protein 7, green (phalloidin is shown in blue). The correct medial-lateral patterning of cochlear hair cells and supporting cells to form the precise rows shown is essential for auditory function, and depends in part on the transmembrane protein encoded by *Leucine Rich Repeat Neuronal 1*.

Credits: Helen R. Maunsell, Kathryn Ellis, Matthew W. Kelley and Elizabeth Carroll Driver

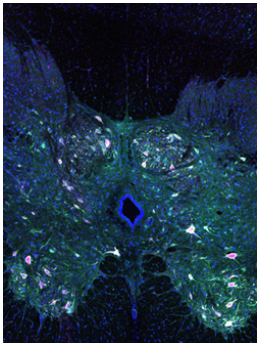
Journal of Neuroscience 19 July 2023, 43 (29) 5305-5318; DOI:
<https://doi.org/10.1523/JNEUROSCI.2141-22.2023>



Description: The nuclei of neural stem and progenitor cells are marked by the expression of nuclear-localized cyan fluorescent protein (CFP). In this issue, Amelchenko et al. present a novel behavioral task and show that ablation of neural stem cells using gamma-irradiation, while sparing learning and memory, selectively impairs cognitive flexibility. They also show that distinct components of the task activate cohorts of newly generated neurons that were born three months earlier, suggesting a significantly extended critical period during which adult-born neurons exhibit augmented plasticity.

Credits: Evgeny M. Amelchenko, Dmitri V. Bezriadnov, Olga A. Chekhov, Anna A. Ivanova, Alexander V. Kedrov, Konstantin V. Anokhin, Alexander A. Lazutkin and Grigori Enikolopov

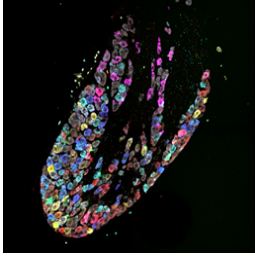
Journal of Neuroscience 23 August 2023, 43 (34) 6061-6083; DOI:
<https://doi.org/10.1523/JNEUROSCI.0161-22.2023>



Description: Immunofluorescent image of a cross section of a non-human primate (*Macaca fascicularis*) spinal cord, dosed intravenously with HSC15/ARSA-V5 gene therapy vector demonstrating successful ARSAV5 expression (magenta) in cells, including neurons and glia, that endogenously express cynomolgus Arsa (green) and where colocalization of both signals appears in white. The detection of an ARSA-V5 signal in the spinal cord confirms that HSC15/ARSA-V5 crossed the blood-brain barrier in larger species.

Credits: Thia St. Martin, Tania A. Seabrook, Katherine Gall, Jenn Newman, Nancy Avila, April Hayes, Monicah Kivaa, Jason Lotterhand, Michael Mercaldi, Kruti Patel, Israel J. Rivas, Stephen Woodcock, Teresa L. Wright, Albert B. Seymour, Omar L. Francone and Jacinthe Gingras

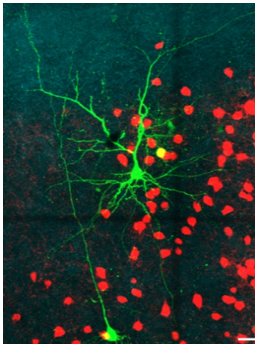
Journal of Neuroscience 10 May 2023, 43 (19) 3567-3581; DOI:
<https://doi.org/10.1523/JNEUROSCI.1829-22.2023>



Title: Ontogeny and Trophic Factor Sensitivity of Gastrointestinal Projecting Vagal Sensory Cell Types

Authors: Meaghan E. McCoy and Anna K. Kamitakahara

<https://doi.org/10.1523/ENEURO.0511-22.2023>. Published March 27, 2023.

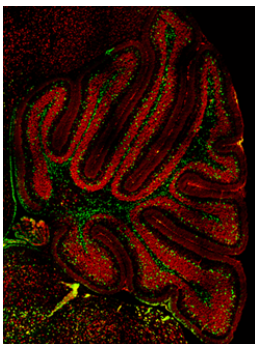


Title: Correlated Somatosensory Input in Parvalbumin/Pyramidal Cells in Mouse Motor Cortex

Authors: Roman U. Goz and Bryan M. Hooks

<https://doi.org/10.1523/ENEURO.0488-22.2023> Published April 24, 2023

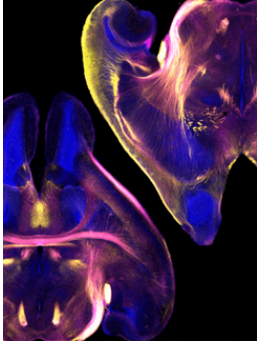
Photo Booth Backgrounds



Description: The image shows a postnatal mouse cerebellum stained for Pax2 (green) and NeuN (red), highlighting immature inhibitory interneurons and excitatory granule cells, respectively. Shh signaling promotes the expansion of Pax2 progenitors that contribute selectively to the stellate cell pool, one of two molecular layer interneuron subtypes.

Credits: Wen Li, Lei Chen, Jonathan T. Fleming, Emily Brignola, Kirill Zavalin, Andre Lagrange, Tonia Rex, Shane A. Heiney, Gregory J. Wojaczynski, Javier F. Medina and Chin Chiang

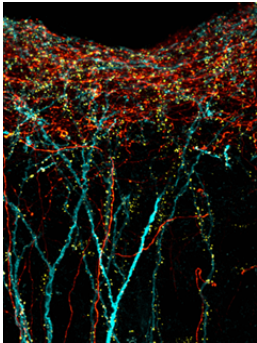
Journal of Neuroscience 29 June 2022, 42 (26) 5130-5143; DOI:
<https://doi.org/10.1523/JNEUROSCI.2073-21.2022>



Description: This image shows horizontal brain sections from a neonatal wild-type mouse (bottom left) and a Tbr1 knockout mouse (top right), immunostained for the axon markers L1 (magenta) and neurofilament medium chain (yellow) with a nuclear counterstain (blue). Homozygous Tbr1 mutation causes severe axon tract defects and upregulation of neurofilament.

Credits: Marissa Co, Rebecca A. Barnard, Jennifer N. Jahncke, Sally Grindstaff, Lev M. Fedorov, Andrew C. Adey, Kevin M. Wright and Brian J. O'Roak

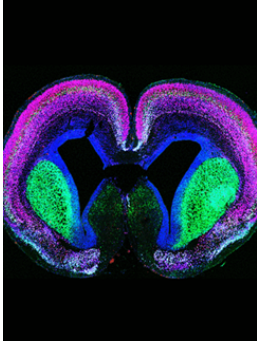
Journal of Neuroscience 14 September 2022, 42 (37) 7166-7181; DOI:
<https://doi.org/10.1523/JNEUROSCI.0409-22.2022>



Description: Superficial layers of mouse primary somatosensory cortex showing apical dendrites of L5 pyramidal neurons labeled with a cyan fluorescent protein (CFP)-cell fill, and excitatory post-synaptic sites marked by PSD95.FingR-Citrine (yellow). Higher order thalamic (posterior medial nucleus, P0m) axons innervating L1 are labeled with tdTomato (red) to enable digital detection of thalamocortical synapses onto L5 dendrites.

Credits: Ajit Ray, Joseph A. Christian, Matthew B. Mosso, Eunsol Park, Waja Wegner, Katrin I. Willig and Alison L. Barth

Journal of Neuroscience 25 January 2023, 43 (4) 584-600; DOI:
<https://doi.org/10.1523/JNEUROSCI.1372-22.2022>

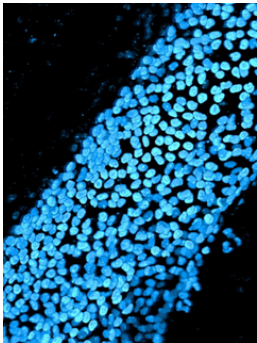


Description: This image shows a section of brain from an embryonic day 18 (E18) mouse lacking the motile cilia gene *Ccdc39*. These mice develop progressive hydrocephalus starting at postnatal day 1, with thinning of layers II-IV by postnatal day 8, but at E18, cortical layers are well retained, as indicated by staining with markers of layers II-IV (SATB2; red), layer V (CTIP2; green), and layer VI (TBR1; purple).

Credits: Eri Iwasawa, Farrah N. Brown, Crystal Shula, Fatima Kahn, Sang Hoon Lee, Temugin Berta, David R. Ladle, Kenneth Campbell, Francesco T. Mangano and June Goto

Journal of Neuroscience 2 March 2022, 42 (9) 1820-1844; DOI: <https://doi.org/10.1523/JNEUROSCI.1160-21.2021>

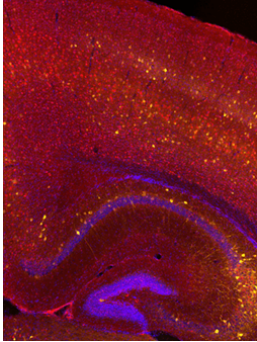
Puzzles



Description: The nuclei of neural stem and progenitor cells are marked by the expression of nuclear-localized cyan fluorescent protein (CFP). In this issue, Amelchenko et al. present a novel behavioral task and show that ablation of neural stem cells using gamma-irradiation, while sparing learning and memory, selectively impairs cognitive flexibility. They also show that distinct components of the task activate cohorts of newly generated neurons that were born three months earlier, suggesting a significantly extended critical period during which adult-born neurons exhibit augmented plasticity.

Credits: Evgeny M. Amelchenko, Dmitri V. Bezriadnov, Olga A. Chekhov, Anna A. Ivanova, Alexander V. Kedrov, Konstantin V. Anokhin, Alexander A. Lazutkin and Grigori Enikolopov

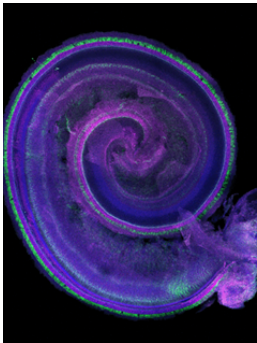
Journal of Neuroscience 23 August 2023, 43 (34) 6061-6083; DOI: <https://doi.org/10.1523/JNEUROSCI.0161-22.2023>



Description: This image shows parvalbumin (yellow), β -catenin (red), and DAPI (blue) in an APC cKO mouse. In their article, Ryner et al. show that the maturation and survival of parvalbumin interneurons are disrupted in a model of early life epilepsy, known as infantile spasms. Inhibitory circuits are prominently shaped by development, so early life seizures may disrupt parvalbumin interneuron maturation. Conversely, inhibitory circuit dysfunction may contribute to seizure initiation, creating a potentially vicious cycle. By combining genetic models of infantile spasms, with anatomical and electrophysiological approaches, the authors shed new light on potential mechanisms of pathogenesis in a model of devastating early life epilepsy.

Credits: Rachael F. Ryner, Isabel D. Derera, Moritz Armbruster, Anar Kansara, Mary E. Sommer, Antonella Pirone, Farzad Noubary, Michele Jacob and Chris G. Dulla

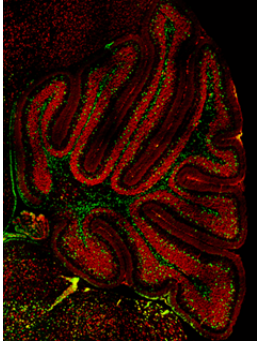
Journal of Neuroscience 22 February 2023, 43 (8) 1422-1440; DOI:
<https://doi.org/10.1523/JNEUROSCI.0572-22.2022>



Description: Surface view of a neonatal mouse cochlea, from tiled confocal projection images. Mechanosensory hair cells are labeled with Myosin VIIa, magenta, and a subset of supporting cells are labeled with Fatty acid binding protein 7, green (phalloidin is shown in blue). The correct medial-lateral patterning of cochlear hair cells and supporting cells to form the precise rows shown is essential for auditory function, and depends in part on the transmembrane protein encoded by *Leucine Rich Repeat Neuronal 1*.

Credits: Helen R. Maunsell, Kathryn Ellis, Matthew W. Kelley and Elizabeth Carroll Driver

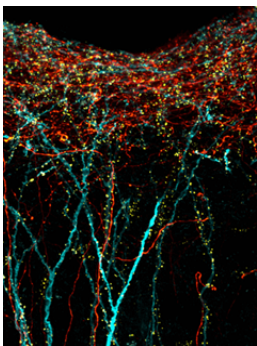
Journal of Neuroscience 19 July 2023, 43 (29) 5305-5318; DOI:
<https://doi.org/10.1523/JNEUROSCI.2141-22.2023>



Description: The image shows a postnatal mouse cerebellum stained for Pax2 (green) and NeuN (red), highlighting immature inhibitory interneurons and excitatory granule cells, respectively. Shh signaling promotes the expansion of Pax2 progenitors that contribute selectively to the stellate cell pool, one of two molecular layer interneuron subtypes.

Credits: Wen Li, Lei Chen, Jonathan T. Fleming, Emily Brignola, Kirill Zavalin, Andre Lagrange, Tonia Rex, Shane A. Heiney, Gregory J. Wojaczynski, Javier F. Medina and Chin Chiang

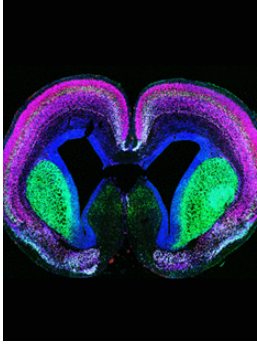
Journal of Neuroscience 29 June 2022, 42 (26) 5130-5143; DOI:
<https://doi.org/10.1523/JNEUROSCI.2073-21.2022>



Description: Superficial layers of mouse primary somatosensory cortex showing apical dendrites of L5 pyramidal neurons labeled with a cyan fluorescent protein (CFP)-cell fill, and excitatory post-synaptic sites marked by PSD95.FingR-Citrine (yellow). Higherorder thalamic (posterior medial nucleus, P0m) axons innervating L1 are labeled with tdTomato (red) to enable digital detection of thalamocortical synapses onto L5 dendrites.

Credits: Ajit Ray, Joseph A. Christian, Matthew B. Mosso, Eunsol Park, Waja Wegner, Katrin I. Willig and Alison L. Barth

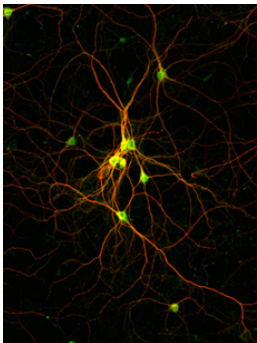
Journal of Neuroscience 25 January 2023, 43 (4) 584-600; DOI:
<https://doi.org/10.1523/JNEUROSCI.1372-22.2022>



Description: This image shows a section of brain from an embryonic day 18 (E18) mouse lacking the motile cilia gene *Ccdc39*. These mice develop progressive hydrocephalus starting at postnatal day 1, with thinning of layers II-IV by postnatal day 8, but at E18, cortical layers are well retained, as indicated by staining with markers of layers II-IV (SATB2; red), layer V (CTIP2; green), and layer VI (TBR1; purple).

Credits: Eri Iwasawa, Farrah N. Brown, Crystal Shula, Fatima Kahn, Sang Hoon Lee, Temugin Berta, David R. Ladle, Kenneth Campbell, Francesco T. Mangano and June Goto

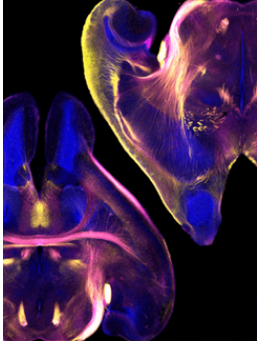
Journal of Neuroscience 2 March 2022, 42 (9) 1820-1844; DOI:
<https://doi.org/10.1523/JNEUROSCI.1160-21.2021>



Description: The image shows cultured neurons from mouse cortex labeled with the dendritic marker protein MAP-2 (red) and the protein kinase SLK (green). In neuronal cells, SLK regulates the formation of the distal dendritic tree and the stabilization of inhibitory synapses.

Credits: Susanne Schoch, Anne Quatraccioni, Barbara K. Robens, Robert Maresch, Karen M.J. van Loo, Silvia Cases-Cunillera, Tony Kelly, Thoralf Opitz, Valeri Borger, Dirk Dietrich, Julika Pitsch, Heinz Beck and Albert J. Becker

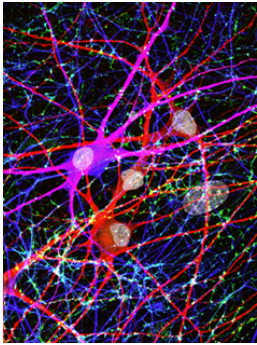
Journal of Neuroscience 29 September 2021, 41 (39) 8111-8125; DOI:
<https://doi.org/10.1523/JNEUROSCI.0352-21.2021>



Description: This image shows horizontal brain sections from a neonatal wild-type mouse (bottom left) and a Tbr1 knockout mouse (top right), immunostained for the axon markers L1 (magenta) and neurofilament medium chain (yellow) with a nuclear counterstain (blue). Homozygous Tbr1 mutation causes severe axon tract defects and upregulation of neurofilament.

Credits: Marissa Co, Rebecca A. Barnard, Jennifer N. Jahncke, Sally Grindstaff, Lev M. Fedorov, Andrew C. Adey, Kevin M. Wright and Brian J. O'Roak

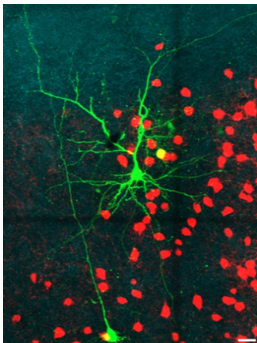
Journal of Neuroscience 14 September 2022, 42 (37) 7166-7181; DOI:
<https://doi.org/10.1523/JNEUROSCI.0409-22.2022>



Description: This confocal image depicts neurons that were derived from human stem cells and sparsely infected with lentivirus expressing EGFP (blue). Nuclei were labeled with DAPI (white), dendrites labeled with antibodies against MAP2 (red), and synapses labeled with antibodies against synapsin (green). These neurons were used to assess phenotypes resulting from a mutation in the synaptic organizing protein Neuroligin-4.

Credits: Thomas P. Cast, Daniel J. Boesch, Kim Smyth, Alisa E. Shaw, Michael Ghebrial and Soham Chanda

Journal of Neuroscience 20 January 2021, 41 (3) 392-407; DOI:
<https://doi.org/10.1523/JNEUROSCI.0404-20.2020>

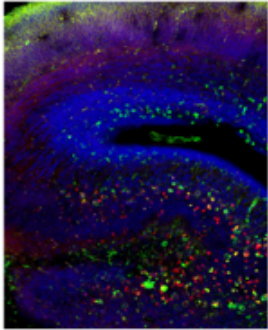


Title: Correlated Somatosensory Input in Parvalbumin/Pyramidal Cells in Mouse Motor Cortex

Authors: Roman U. Goz and Bryan M. Hooks

<https://doi.org/10.1523/ENEURO.0488-22.2023> Published April 24, 2023

Signage

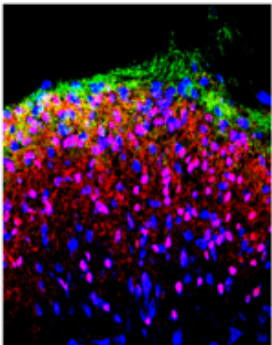


Description: Munc 18-1 knock-out mouse brain (E18) showing cellular stress response in hippocampus and cortex by phosphorylated p53 staining (green) and cell death in the hippocampus marked by fragmented cleaved caspase 3 (red) positive nuclei (DAPI in blue).

Credits: Femke M. Feringa, Annemiek A. van Berkel, Anushka Nair and Matthijs Verhage

Journal of Neuroscience 18 January 2023, 43 (3) 347-358; DOI: <https://doi.org/10.1523/JNEUROSCI.0611-22.2022>

PRODUCT THEATER - EXHIBIT HALL

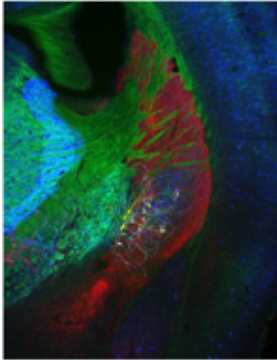


Description: This image shows the distribution of μ -opioid receptors (green) among neurons labeled with NeuN (blue) and neurons expressing tdTomatotagged vesicular glutamate transporter-2 (red) in the mouse spinal dorsal horn.

Credits: Shao-Rui Chen (陈少瑞), Hong Chen (陈红), Daozhong Jin (金道忠) and Hui-Lin Pan (潘惠麟)

Journal of Neuroscience 14 December 2022, 42 (50) 9315-9329; DOI: <https://doi.org/10.1523/JNEUROSCI.1704-22.2022>

ATTENDEE SERVICES - EAST SALON

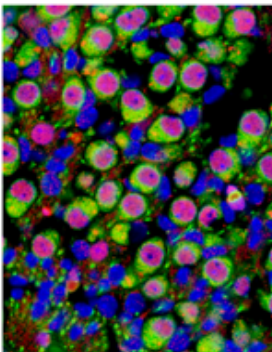


Description: Reconstructions of GABAergic neurons of a novel large type accumulating in the tail of the striatum (TS). They are detectable using a neurofilament marker SMI-32 (green) and parvalbumin immunohistochemistry (blue). These TSL (TS large) neurons elongate skewed dendrites toward the region where dopaminergic axons (red) are relatively sparse. Importantly, this region selectively receives inputs from the primary auditory cortex.

Credits: Shigeru Ogata, Yuta Miyamoto, Naoki Shigematsu, Shigeyuki Esumi and Takaichi Fukuda

Journal of Neuroscience 26 October 2022, 42 (43) 8078-8094; DOI:
<https://doi.org/10.1523/JNEUROSCI.2236-21.2022>

SfN INFO COUNTERS - GRAND LOBBY & L STREET

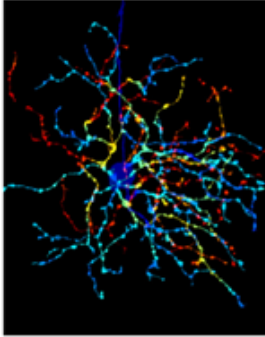


Description: This image shows expression of MEF2C protein (purple) in nuclei of type I spiral ganglion neurons (Class III β -TUBULIN⁺; green) in the young adult mouse auditory nerve. Nuclei were stained with Dapi (blue).

Credits: Nathan McChesney, Jeremy L. Barth, Jeffrey A. Rumschlag, Junying Tan, Adam J. Harrington, Kenyaria V. Noble, Carolyn M. McClaskey, Phillip Elvis, Silvia G. Vaena, Martin J. Romeo, Kelly C. Harris, Christopher W. Cowan and Hainan Lang

Journal of Neuroscience 19 October 2022, 42 (42) 8002-8018; DOI:
<https://doi.org/10.1523/JNEUROSCI.0253-22.2022>

LANYARD BIN, PRONOUN STICKER BAR



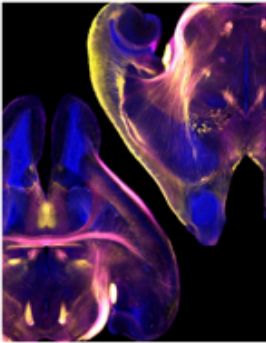
Description: This image shows a transient Suppressed-by-Contrast ganglion cell whose dendrites are colored according to their depth in the retina.

Credits: Nai-Wen Tien, Carmela Vitale, Tudor C. Badea and Daniel Kerschensteiner

Journal of Neuroscience 21 September 2022, 42 (38) 7213-7221; DOI:

<https://doi.org/10.1523/JNEUROSCI.2332-21.2022>

EXHIBIT HALL ENTRANCE



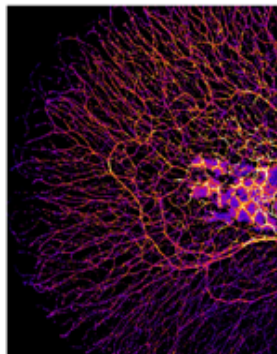
Description: This image shows horizontal brain sections from a neonatal wild-type mouse (bottom left) and a Tbr1 knockout mouse (top right), immunostained for the axon markers L1 (magenta) and neurofilament medium chain (yellow) with a nuclear counterstain (blue). Homozygous Tbr1 mutation causes severe axon tract defects and upregulation of neurofilament.

Credits: Marissa Co, Rebecca A. Barnard, Jennifer N. Jahncke, Sally Grindstaff, Lev M. Fedorov, Andrew C. Adey, Kevin M. Wright and Brian J. O'Roak

Journal of Neuroscience 14 September 2022, 42 (37) 7166-7181; DOI:

<https://doi.org/10.1523/JNEUROSCI.0409-22.2022>

SHUTTLE INFORMATION

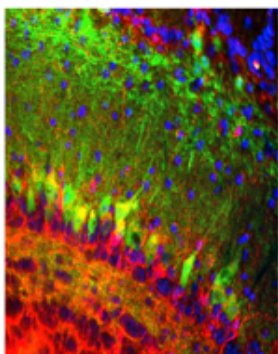


Description: This image shows a Z-projection of all the sensory axon arbors that innervate the skin of a larval zebrafish tail and the differential activation of Src Family Kinases (SFKs) within those axons. Immunostaining for phosphorylated SFK in transgenically-labeled somatosensory axons combined with 3D image analysis allows visualization of different levels of SFK activity within portions of the axon from high levels (white/red/orange) to low levels (purple/blue). Tuttle et al. identify a new role for SFKs in the maintenance of these sensory axons within the skin.

Credits: Adam M. Tuttle, Matthew B. Pomaville, Katherine C. Delgado, Kevin M. Wright and Alex V. Nechiporuk

Journal of Neuroscience 7 September 2022, 42 (36) 6835-6847; DOI:
<https://doi.org/10.1523/JNEUROSCI.0618-22.2022>

EXHIBIT HALL DIRECTORY AND PROGRAM & EXHIBIT GUIDE PICKUP

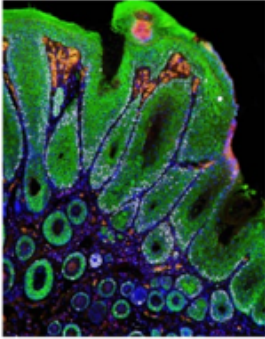


Description: This photomicrograph reflects the experimental power of CRISPR/Cas9 genome editing. Tbx21-Cre mice were bred to a Cas9 line with a GFP reporter and then gRNA targeting the voltage dependent potassium channel, Kv1.3, was retroorbitally delivered. The CRISPR-associated Cas9 protein is restricted to the mitral and tufted output neurons of the olfactory bulb (green) allowing the CRISPR guide RNA (red) to edit the channel from the genome in the target neurons (yellow). This confers the mouse with enhanced olfaction and resistance to diet-induced obesity.

Credits: Louis John Kolling, Roberta Tatti, Troy Lowry, Ashley M. Loeven, James M. Fadool and Debra Ann Fadool

Journal of Neuroscience 27 July 2022, 42 (30) 5966-5990; DOI:
<https://doi.org/10.1523/JNEUROSCI.0190-22.2022>

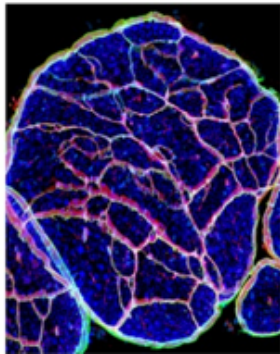
BADGE PICKUP - WEST SALON, CUSTOMER SERVICE



Description: This image shows keratinocytes (green), proliferating cells (white), inflammatory cells (red), and cell nuclei (blue) associated with a skin tumor in a one-year-old mouse lacking PTEN, a protein that regulates cell growth and proliferation. Although loss of PTEN is associated with several cancers, it can also promote axon regeneration in the CNS and PNS.

Credits: Sofia Meyer zu Reckendorf, Diana Moser, Anna Blechschmidt, Venkata Neeha Joga, Daniela Sinske, Jutta Hegler, Stefanie Deininger, Alberto Catanese, Sabine Vettorazzi, Gregor Antoniadis, Tobias Boeckers and Bernd Knöll

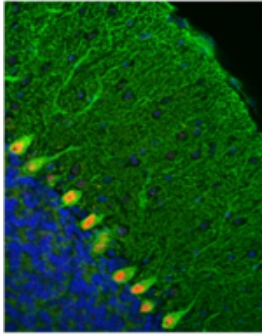
Journal of Neuroscience 23 March 2022, 42 (12) 2474-2491; DOI:
<https://doi.org/10.1523/JNEUROSCI.1305-21.2022>



Description: Confocal image of a section of sciatic nerve from an adult mouse lacking Gli-1, a transcription factor expressed in the endoneurial compartment of peripheral nerves independent of its canonical activator, the Hedgehog pathway. Fate mapping with Gli1-Cre (red) labels both the perineurium, which surrounds the nerve exterior, and cells forming minifascicles, structures that aberrantly subdivide these knockout peripheral nerves into multiple small compartments. The nerve is additionally stained for axonal neurofilament (blue) and the glucose transporter Glut-1 (green).

Credits: Brendan Zotter, Or Dagan, Jacob Brady, Hasna Baloui, Jayshree Samanta and James L. Salzer

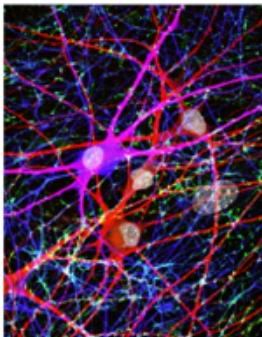
Journal of Neuroscience 12 January 2022, 42 (2) 183-201; DOI:
<https://doi.org/10.1523/JNEUROSCI.3096-20.2021>



Description: This image shows accumulation of polyglutamine-expanded ATXN7 (red) in CALB1-immunostained Purkinje neurons (green) in cerebellum in a mouse model of spinocerebellar ataxia type 7. This abnormal accumulation leads to the progressive downregulation of 83 Purkinje identity genes critical for spontaneous firing activity and synaptic functions.

Credits: Anna Niewiadomska-Cimicka, Frédéric Doussau, Jean-Baptiste Perot, Michel J. Roux, Celine Keime, Antoine Hache, Françoise Piguet, Ariana Novati, Chantal Weber, Binnaz Yalcin, Hamid Meziane, Marie-France Champy, Erwan Grandgirard, Alice Karam, Nadia Messaddeq, Aurélie Eisenmann, Emmanuel Brouillet, Hoa Huu Phuc Nguyen, Julien Flament, Philippe Isope and Yvon Trottier

Journal of Neuroscience 2 June 2021, 41 (22) 4910-4936; DOI:
<https://doi.org/10.1523/JNEUROSCI.1882-20.2021>

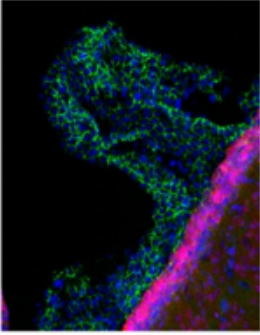


Description: This confocal image depicts neurons that were derived from human stem cells and sparsely infected with lentivirus expressing EGFP (blue). Nuclei were labeled with DAPI (white), dendrites labeled with antibodies against MAP2 (red), and synapses labeled with antibodies against synapsin (green). These neurons were used to assess phenotypes resulting from a mutation in the synaptic organizing protein Neuroligin-4.

Credits: Thomas P. Cast, Daniel J. Boesch, Kim Smyth, Alisa E. Shaw, Michael Ghebrial and Soham Chanda

Journal of Neuroscience 20 January 2021, 41 (3) 392-407; DOI:
<https://doi.org/10.1523/JNEUROSCI.0404-20.2020>

SfN STORE - EAST SALON

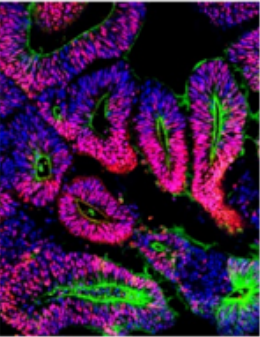


Description: This image shows GFAP-Cre activity (tdTomato/red) in a choroid plexus (marked by β -catenin/green) of a lateral ventricle of mouse brain at postnatal day 7.

Credits: Kong-yan Wu, Fu-lei Tang, Daehoon Lee, Yang Zhao, Hyunjin Song, Xiao-Juan Zhu, Lin Mei and Wen-Cheng Xiong

Journal of Neuroscience 6 May 2020, 40 (19) 3862-3879; DOI:
<https://doi.org/10.1523/JNEUROSCI.1520-19.2020>

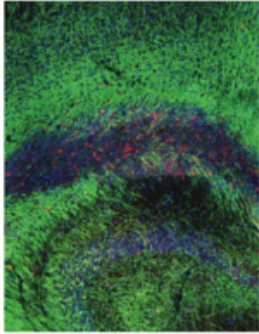
BADGE PICKUP - L STREET CONCOURSE, OUTSIDE 151



Description: This image shows a cross section of a day 28 human forebrain organoid, showing FOXG1-expressing neural precursors (Red), surrounding a ventricle-like structure outlined by N-Cadherin staining (Green). DAPI staining is blue.

Credits: Ai Tian, Julien Muffat and Yun Li

Journal of Neuroscience 5 February 2020, 40 (6) 1186-1193; DOI:
<https://doi.org/10.1523/JNEUROSCI.0519-19.2019>

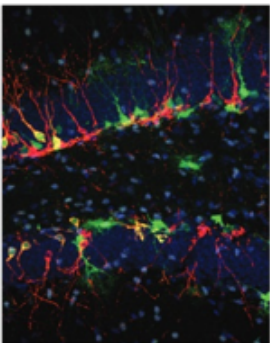


Description: The image shows a portion of the mouse corpus callosum 10 days after focal demyelination by injection with lyssolecithin. The mouse was treated with the pro-remyelinating, selective estrogen receptor modulator bazedoxifene, and it shows clear remyelination, as indicated by immunostaining for myelin oligodendrocyte glycoprotein (green) and increased numbers of oligodendrocytes (red) within the lesion borders. Cell nuclei were identified by DAPI (blue).

Credits: Kelsey A. Rankin, Feng Mei, Kicheol Kim, Yun-An A. Shen, Sonia R. Mayoral, Caroline Despons, Daniel S. Lorrain, Ari J. Green, Sergio E. Baranzini, Jonah R. Chan and Riley Bove

Journal of Neuroscience 20 March 2019, 39 (12) 2184-2194; DOI:
<https://doi.org/10.1523/JNEUROSCI.1530-18.2019>

Neurojobs

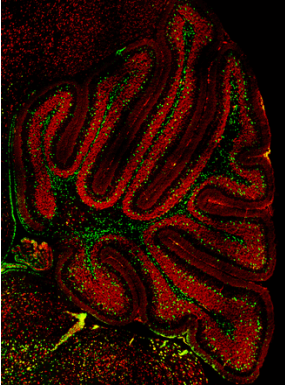


Description: This image shows the mouse adult hippocampus with neurogenesis markers. EYFP (green) is expressed in radial glia-like neural stem cells and their progenies. Adult-born neurons and neural stem cells/neural progenitors are stained with Doublecortin (red) and Sox2 (white), respectively. DAPI labeling is blue.

Credits: H. Georg Kuhn, Tomohisa Toda and Fred H. Gage

Journal of Neuroscience 5 December 2018, 38 (49) 10401-10410; DOI:
<https://doi.org/10.1523/JNEUROSCI.2144-18.2018>

PROGRAM & EXHIBIT GUIDE, SIGNAGE, L STREET BRIDGE TOWER - METRO ENTRANCE



Description: The image shows a postnatal mouse cerebellum stained for Pax2 (green) and NeuN (red), highlighting immature inhibitory interneurons and excitatory granule cells, respectively. Shh signaling promotes the expansion of Pax2 progenitors that contribute selectively to the stellate cell pool, one of two molecular layer interneuron subtypes.

Credits: Wen Li, Lei Chen, Jonathan T. Fleming, Emily Brignola, Kirill Zavalin, Andre Lagrange, Tonia Rex, Shane A. Heiney, Gregory J. Wojaczynski, Javier F. Medina and Chin Chiang

Journal of Neuroscience 29 June 2022, 42 (26) 5130-5143; DOI:
<https://doi.org/10.1523/JNEUROSCI.2073-21.2022>